

UNPUBLISHED PRELIMINARY DATA

CRITERIA FOR EMITTER SHEATH POLARITY IN PLASMA DIODES*

George L. Schrenk

Institute for Direct Energy Conversion; Towne School of Civil and Mechanical Engineering; University of Pennsylvania; Philadelphia, Pa.

Abstract

15376

The general criteria used to determine the sign (polarity) of the emitter sheath in a plasma diode are examined in detail. It is shown that these general criteria reduce to those criteria presently in common use only for a collisionless plasma diode. For a broad-spaced collision dominated plasma diode, however, a phenomenological macroscopic model is used to show that the ratio of the electron emission current to the ion emission current does not uniquely determine the polarity of the emitter sheath. The net volume ionization and/or recombination and the electron plasma temperature are also shown to be important. No specific mechanism for volume ionization is assumed; both the net volume ionization and the electron temperature are treated as unknown parameters. Numerical results are presented for several cases of interest in thermionic energy conversion.

author

N 65 15376

(ACCESSION NUMBER)

31

(PAGES)

CP 60333

(NASA CR OR TMX OR AD NUMBER)

(THRU)

1

(CODE)

25

(CATEGORY)

GPO PRICE \$

OTS PRICE(S) \$

Hard copy (HC)

2.00

Microfiche (MF)

.50

*This research was supported by NASA Contract NSG-316 to the Institute for Direct Energy Conversion, Towne School of Civil and Mechanical Engineering, University of Pennsylvania.

Introduction

The criteria presently used for determining the sign of the emitter sheath in both close- and broad-spaced cesium plasma diodes are

$I_s/I_{pE} > 491 \Rightarrow$ electron rich (negative) emitter sheath,

$I_s/I_{pE} < 491 \Rightarrow$ ion rich (positive) emitter sheath,

where I_s is the electron emission current (as given by the Richardson equation) and I_{pE} is the ion current from the emitter. It will be shown in the next section that these criteria follow directly from a more general set of criteria by assuming that no collisions occur in the interelectrode space. Thus, the applicability of these criteria to a close-spaced collisionless diode cannot be questioned.

In a broad-spaced plasma diode, however, there are interactions in the interelectrode space and these interactions give rise to volume ionization and/or recombination. Since the presence of volume ionization in the interelectrode space of a plasma diode modifies the potential distribution, it must also enter into the determination of the emitter sheath sign. The criteria stated above, however, do not take into account such effects.

A phenomenological macroscopic model has been used to determine the correct criteria when interactions exist in the interelectrode space. Specifically, this model applies to a broad-spaced plasma diode where the spacing is many times the mean free path—i.e., to the case where a plasma, characterized by its own variables, is formed in the interelectrode space. No specific mechanism for volume ionization and/or recombination is assumed; both the net volume ionization and the plasma electron temperature are treated as unknown parameters. Plasma resistivity has been neglected. In

this paper the equations that describe this model will be derived and the assumptions that were made will be discussed. The procedures employed for the solution of this model will be covered and results will be presented for several cases of interest in thermionic energy conversion.

Theoretical Model

Let I_s denote the electron emission current from the emitter surface. This current can be calculated from the Richardson equation if the concept of a work function is introduced. Since no quantitative current-voltage characteristics will be considered in this work, it is never necessary to introduce the concept of a work function. Instead, it is more desirable to work directly in terms of the electron emission current. Let I_{s0} be the electron emission current from the emitter surface when the emitter sheath potential vanishes. The motive diagram for this case is shown in Figure 1.

Using these definitions, the general criteria for determining the polarity of the emitter sheath can be written as

$$I_s > I_{s0} \Rightarrow \text{electron rich (negative) emitter sheath,}$$

$$I_s < I_{s0} \Rightarrow \text{ion rich (positive) emitter sheath.}$$

These criteria readily follow from fundamental physical principles and are valid for all operating regimes in both close- and broad-spaced plasma diodes.

For a close-spaced diode (no interactions in the interelectrode space), these general criteria readily reduce to the criteria stated in the preceding section. To see this, it is only necessary to introduce the concept of charge neutrality in a plasma with equal electron and ion temperatures: $I_s = \sqrt{m_p/m_e} I_{pE} = 491 I_{pE}$. Since there are no interactions in the interelectrode space (and

thus no reverse electron and ion currents), it follows that *

$I_s/I_{pE} > 491 \Rightarrow$ electron rich (negative) emitter sheath,

$I_s/I_{pE} < 491 \Rightarrow$ ion rich (positive) emitter sheath.

These criteria hold for the close-spaced collisionless plasma diode.

Whenever interactions are present, I_{so} cannot be written down so easily. Interactions give rise to electron and ion currents returning from the plasma to the emitter surface; thus I_{so} must be a function of such currents. The calculation of these reverse currents requires a specific model.

A phenomenological macroscopic model will be used to determine the values of I_{so} for a broad-spaced plasma diode where the spacing is many times the mean free path—i.e., for the case where a plasma, characterized by its own variables, is formed in the interelectrode space. In order that this model remain as general as possible, the electron temperature V_{Te} and the net volume ionization and/or recombination A_{DE} have been chosen to be unknown parameters. Thus no specific ionization rates have been assumed. The basic assumptions used in this model are:

1. The temperature of the collector is low so that electron and ion generation at the collector are negligible.
2. The Saha-Langmuir equation is a valid representation of ion generation at the emitter surface. This equation, however, has been rewritten so as to use the electron emission current I_{so} explicitly; thus the concept of an emitter work function is never explicitly introduced.
3. The plasma in the interelectrode space is uniform with the ion density equal to the electron density throughout.
4. Maxwellian distributions of electrons and ions exist in the plasma; the corresponding electron and gas temperatures, however, need not be equal.
5. Plasma resistance is neglected.

*It is important to emphasize that this result is independent of the question of the validity of the Saha-Langmuir equation. The Saha-Langmuir equation enters only if one attempts to calculate I_{pE} in terms of I_s (or the emitter work function).

6. Extraneous losses, such as thermal radiation from the plasma to the surroundings, loss of electrons, ions, and atoms from the interelectrode space, are neglected.
7. Only two species of cesium are considered to exist in the plasma—atoms and ions. No provisions are presently made for the possible existence of excited atoms and/or molecules.

Using these assumptions, a set of six simultaneous equations have been formulated to describe the condition when the emitter sheath vanishes. A brief derivation of each equation follows:

For the current balance at the emitter surface, the net current I is the result of four groups of charge carriers: (1) saturation current from the emitter I_{so} ; (2) ion current from the emitter I_{pE} ; (3) electrons from the plasma (reverse electron current) I_{ep} ; and (4) ions from the plasma (reverse ion current) I_p . Thus

$$I = I_{so} - I_{pE} + I_p - I_{ep}. \quad (1)$$

For the current balance at the collector surface, the net current I is the result of only two groups of charge carriers: (1) electrons from the plasma $I_{ep} \exp(-V_{SC}/V_{Te})$; and (2) ions from the plasma I_p , where V_{Te} denotes the electron plasma temperature. The collector sheath is always assumed to be positive in this model.

Thus

$$I = I_{ep} \exp(-V_{SC}/V_{Te}) - I_p. \quad (2)$$

The equation for the ion balance across the plasma is

$$I_{pE} + A_{DE} = 2I_p, \quad (3)$$

where A_{DE} is the net volume ionization and/or recombination in amps/cm².

The equation for the ion production at the emitter is

$$I_{pE} = I_a / [1 + 2I_{so} \exp(V_i/V_{TE})/AT_E^2] , \quad (4)$$

where I_a = arrival rate of atoms and ions from the plasma,
 V_i = ionization potential of cesium,
 V_{TE} = emitter temperature (ev),
 A = thermionic emission constant (120 amps/cm²).

This is the Saha-Langmuir equation, rederived in a manner such that the concept of an emitter work function is never explicitly introduced.

The equation for the charge density balance in the plasma is

$$I_{ep} \sqrt{m_e/V_{Te}} = I_p \sqrt{m_p/V_G} \quad (5)$$

where V_G denotes the gas temperature (ev).

The equation for the energy balance for the plasma is

$$\begin{aligned} 2I_{so} (V_{TE} - V_{Te}) + 2I_a (V_{TE} + V_{TC} - 2V_G) \\ - A_{DE} (V_i + 2V_{Te}) - (I + I_p)V_{SC} = 0 \end{aligned} \quad (6)$$

where V_{TC} is the collector temperature (ev). Although the approach used to obtain this equation is similar to that employed in Reference 1, the reference points and grouping of terms used are fundamentally different.* This equation expresses the fact that the net energy flowing across an imaginary surface immediately outside the

*These differences are significant as it is not necessary to introduce detailed interaction mechanisms to evaluate any of the terms occurring in this energy balance equation.

emitter must equal the net energy flowing across a similar imaginary surface immediately outside the collector when the same potential reference points are used for both imaginary surfaces. Since only ions and atoms are considered to be crossing these imaginary surfaces, the possible presence of excited atoms and/or molecules has been neglected. A derivation of this equation is presented in the Appendix.

In order to study the solution of this set of six simultaneous non-linear equations, it is convenient to rewrite these equations in a different form. Substituting Equations (1), (2), (3), and (5) into Equation (6), it follows that

$$\begin{aligned}
 & 2I_{s0}(V_{TE} - V_{Te}) + 2I_a(V_{TE} + V_{TC} - 2V_G) - A_{DE}(V_i + 2V_{Te}) \\
 & = \left[I_{s0} + A_{DE} \left(1 - \frac{1}{2} \sqrt{m_p V_{Te} / m_e V_G} \right) - \frac{I_{pE}}{2} \sqrt{m_p V_{Te} / m_e V_G} \right] V_{sc}
 \end{aligned} \tag{7}$$

where

$$V_{sc} = -V_{Te} \ln \left\{ \frac{2 \left[I_{s0} + A_{DE} \left(1 - \frac{1}{2} \sqrt{m_p V_{Te} / m_e V_G} \right) - \frac{I_{pE}}{2} \sqrt{m_p V_{Te} / m_e V_G} \right]}{(I_{pE} + A_{DE}) \sqrt{m_p V_{Te} / m_e V_G}} \right\}$$

and where Equation (4) continues to be used to relate I_{pE} to V_{Te} . It is convenient to look for solutions of this equation in the $I_s - A_{DE}$ plane with V_{Te} treated as a parameter. A study of Equation (7) in the $I_s - A_{DE}$ plane shows that this equation possesses solutions only in very limited ranges. These restricted ranges can be found as follows:

Physically, it is necessary that $I_p \geq 0$. From Equation (3), it follows that $A_{DE} \geq -I_{pE}$. Also, $0 \leq V_{SC} \leq \infty$. Thus, from Equation (7), it follows that

$$I_{so} + A_{DE} \left(1 - \frac{1}{2} \sqrt{m_p V_{Te} / m_e V_G}\right) - \frac{I_{pE}}{2} \sqrt{m_p V_{Te} / m_e V_G} \geq 0 \quad (8)$$

and

$$2 \left[I_{so} + A_{DE} \left(1 - \frac{1}{2} \sqrt{m_p V_{Te} / m_e V_G}\right) - \frac{I_{pE}}{2} \sqrt{m_p V_{Te} / m_e V_G} \right] \leq (I_{pE} + A_{DE}) \sqrt{m_p V_{Te} / m_e V_G}$$

This last inequality can be rewritten as

$$I_{so} + A_{DE} \left(1 - \sqrt{m_p V_{Te} / m_e V_G}\right) - I_{pE} \sqrt{m_p V_{Te} / m_e V_G} \leq 0 \quad (9)$$

Now the equality in Equation (8) gives rise to a bound on I_{so} as a function of A_{DE} . Let this bound, which results when $V_{SC} \rightarrow \infty$, be denoted by $(I_{so})_{\min}$. The equality in Equation (9) also gives rise to a bound on I_{so} as a function of A_{DE} . Let this bound, which results when $V_{SC} \rightarrow 0$, be denoted by $(I_{so})_{\max}$. It is straightforward to show from Equations (8) and (9) that for $(I_{so})_{\max} = (I_{so})_{\min}$, $A_{DE} + I_{pE} = 0$. Since $I_p \geq 0$, it follows from Equation (3) that $A_{DE} + I_{pE} \geq 0$ and thus that $(I_{so})_{\min} \leq (I_{so})_{\max}$. At the point $A_{DE} + I_{pE} = 0$, it can be shown from Equation (3) and Equation (8) that

$$(I_{so})_{\min} \Big|_{A_{DE} + I_{pE} = 0} = -A_{DE} = \frac{-1 + \sqrt{1 + \frac{8I_a}{AT_E^2} \exp(V_i / V_{Te})}}{\frac{4}{AT_E^2} \exp(V_i / V_{Te})} \quad (10)$$

Here the positive root was selected because $I_{so} \geq 0$. This equation serves as a lower bound on both I_{so} and A_{DE} and is independent of V_{Te} .

An upper bound for A_{DE} follows from the left hand side of Equation (7). This bound, however, is not very useful as it is a function of I_{so} and V_{Te} .

Instead of considering further possible bounds on this set of equations, it is convenient to find the envelope of all possible solutions in the $I_s - A_{DE}$ plane. This envelope is given by $(I_{so})_{min}$ from Equation (8) and $(I_{so})_{max}$ from Equation (9). Since each of these equations is a function of two variables, A_{DE} and V_{Te} , it is necessary to have another equation in order to make both $(I_{so})_{min}$ and $(I_{so})_{max}$ functions of one parameter only. Such an equation follows from Equation (7) and the definitions of $(I_{so})_{min}$ and $(I_{so})_{max}$; it can be written as

$$A_{DE} = \frac{2I_{so}(V_{TE} - V_{Te}) + 2I_a(V_{TE} + V_{TC} - 2V_G)}{V_i + 2V_{Te}}$$

Using these equations and defining the following terms

$$a_1 = \frac{2}{AT_E^2} \exp(V_i/V_{TE}) \left[1 + 2 \frac{(1 - \frac{1}{2} \sqrt{m_p V_{Te}/m_e V_G}) (V_{TE} - V_{Te})}{(V_i + 2V_{Te})} \right]$$

$$b_1 = 1 + \frac{(1 - \frac{1}{2} \sqrt{m_p V_{Te}/m_e V_G})}{(V_i + 2V_{Te})} \left[2(V_{TE} - V_{Te}) + \frac{4I_a}{AT_E^2} \exp(V_i/V_{TE}) (V_{TE} + V_{TC} - 2V_G) \right]$$

$$c_1 = \frac{2I_a (1 - \frac{1}{2} \sqrt{m_p V_{Te}/m_e V_G})}{(V_i + 2V_{Te})} (V_{TE} + V_{TC} - 2V_G) - I_a \frac{1}{2} \sqrt{m_p V_{Te}/m_e V_G}$$

$$a_2 = \frac{2}{A_{TE}^2} \exp(V_i/V_{TE}) \left[1 + \frac{2(1 - \sqrt{m_p V_{TE}/m_e V_G})}{(V_i + 2V_{TE})} (V_{TE} - V_{Te}) \right]$$

$$b_2 = 1 + \frac{(1 - \sqrt{m_p V_{TE}/m_e V_G})}{V_i + 2V_{TE}} \left[2(V_{TE} - V_{Te}) + \frac{4I_a}{A_{TE}^2} \exp(V_i/V_{TE}) (V_{TE} + V_{Te} - 2V_G) \right]$$

$$c_2 = \frac{2I_a(1 - \sqrt{m_p V_{TE}/m_e V_G})}{V_i + 2V_{TE}} (V_{TE} + V_{TC} - 2V_G) - I_a \sqrt{m_p V_{TE}/m_e V_G}$$

it can be shown that*

$$(I_{so})_{min} = \frac{-b_1 + \sqrt{b_1^2 - 4a_1c_1}}{2a_1}$$

$$(I_{so})_{max} = \frac{-b_2 + \sqrt{b_2^2 - 4a_2c_2}}{2a_2}$$

These equations describe the envelope of all possible solutions in the $I_s - A_{DE}$ plane as a function of the parameter V_{Te} , where $0 \leq V_{Te} \leq \infty$.

*The plus sign has been chosen for both equations from the requirement that $(I_{so})_{min}$ and $(I_{so})_{max}$ both be greater than zero when $V_{Te} = V_{TE}$.

The envelope for $(I_{so})_{\max}$ has the interesting property that there is a region for which $b_2^2 - 4a_2c_2 < 0$. This region occurs between two regions where $b_2^2 - 4a_2c_2 > 0$ and leads to a discontinuity that occurs in the envelope at infinity. Figure 2 clearly shows the properties of a typical envelope.

All solutions for I_{so} as a function of A_{DE} and V_{Te} lie within the boundaries of this envelope. Physically, however, it is clear that $V_{Te} \geq V_G$. The inclusion of this fact is not simple. A solution for the envelope with the restriction $V_{Te} \geq V_G$ yields a portion of the envelope in Figure 2; but this portion is not closed. To find the closed envelope with the restriction $V_{Te} \geq V_G$ it is also necessary to solve Equation (7) for the solution for $V_{Te} = V_G$. This was done for the same case shown in Figure 2 and the results are shown in Figure 3.

Now, the discontinuity that occurs in the envelope at infinity may occur either for $V_{Te} \geq V_G$ or $V_{Te} < V_G$. Let $(V_{Te})_1$, $(V_{Te})_2$ be the solutions of $b_2^2 - 4a_2c_2 = 0$ with $(V_{Te})_2 \geq (V_{Te})_1$. This discontinuity in the envelope at infinity occurs for $(V_{Te})_2 \geq V_{Te} \geq (V_{Te})_1$. If $(V_{Te})_2 < V_G$, the restricted envelope (i.e., the envelope with $V_{Te} \geq V_G$) is bounded and does not extend to infinity. If $(V_{Te})_2 \geq V_G$, the restricted envelope still possesses the discontinuity at infinity.

The possession of the envelope of all possible solutions of Equation (7) is extremely valuable as the envelope greatly restricts the range over which numerical iterative procedures must search to solve Equation (7). Since A_{DE} and V_{Te} are treated as independent variables, the solutions found for each set of values of T_E , T_C , T_G , and I_a will be a family of curves on a plot of I_s versus A_{DE} . Each curve in this family can be labeled with a value of V_{Te} .

Results

The equations presented in the preceding section have been programmed for solution on an IBM 7040 computer. Figures 4, 5, and 6 show results obtained for $I_a = 1.5 \text{ amps/cm}^2$ ($T_{Cs} \approx 470^\circ\text{K}$), $T_C = 500^\circ\text{K}$, $V_G = \frac{1}{2}(V_{TE} + V_{TC})$, and $T_E = 1400^\circ\text{K}$, 1450°K , 1500°K , respectively. Figures 7, 8, and 9 show results obtained for $I_a = 30.0 \text{ amps/cm}^2$ ($T_{Cs} \approx 565^\circ\text{K}$), $T_C = 500^\circ\text{K}$, $V_G = \frac{1}{2}(V_{TE} + V_{TC})$, and $T_E = 1650^\circ\text{K}$, 1700°K , 1750°K , respectively.

The salient features of these curves are labeled on each figure. The ratio I_s/I_{pE} has been computed at $A_{DE} = 0$ and $V_{SC} = 0, \infty$ and is shown on each curve.* Any broad-spaced plasma diode operating above the top curve in any of these figures necessarily possesses an electron rich (negative) emitter sheath.** Any broad-spaced plasma diode operating below the bottom curve in any of these figures necessarily possesses an ion rich (positive) emitter sheath.** From these figures it is clear that an increase in the net volume ionization with all other parameters constant can cause the operation of such a plasmodiode to go from an electron rich to an ion rich emitter sheath.

For plasma diodes operating in the region between the two curves (i.e., within the restricted envelope) in any of these figures, it is impossible to state whether the emitter sheath is positive or negative without having more information. Although these figures contain part of the full parametric family of curves ($V_G \leq V_{Te} \leq \infty$), it is still necessary to obtain the specific solution that relates A_{DE} to V_{Te} . Only after this precise curve has been specified can conclusions be drawn about the polarity of emitter sheaths for plasma diodes operating in the region between the two curves in these figures.

*It can be shown that for $A_{DE} = 0$: $V_{SC} = 0 \Rightarrow I_s/I_{pE} = \sqrt{m_p V_{Te}/m_e V_G}$; $V_{SC} = \infty \Rightarrow I_s/I_{pE} = \frac{1}{2} \sqrt{m_p V_{Te}/m_e V_G}$. If $V_G = \frac{1}{2}(V_{TE} + V_{TC})$, it can also be shown that $V_{Te} = V_{TE}$ at these two points.

**It must be remembered that these results apply only for $V_{SC} \geq 0$.

Now, the use of the preceding results in the interpretation of current-voltage characteristics is very difficult. These results are given in terms of I_s while experimental measurements yield I . The precise determination of I_s from I is very difficult, if not impossible, in broad-spaced plasma diodes. Thus, it is desirable to develop criteria in terms of I .

From Equations (1), (3), (4), and (5) it can be shown that an I_o , corresponding to I_{so} , can be defined with the property that

$$I > I_o \Rightarrow \text{electron rich (negative) emitter sheath,}$$

$$I < I_o \Rightarrow \text{ion rich (positive) emitter sheath.}$$

Here, however, the envelope corresponding to $(I_{so})_{\min}$ is in the ion current region. Results in terms of I , corresponding to Figures 4-9, are shown in Figures 10-15, respectively. The salient features of these curves are labeled in each figure. These figures show that the reverse current can be a useful diagnostic tool; if the magnitude of the reverse current is large enough, the emitter sheath is ion rich. For plasma diodes operating in the region between the two curves in any of these figures, it is still impossible to state whether the emitter sheath is positive or negative without knowing the relationship between A_{DE} and V_{Te} .

Summary

The general criteria used to determine the sign (polarity) of the emitter sheath in a plasma diode have been examined in detail. It was shown that these general criteria reduce to those criteria presently in common use only for a collisionless plasma diode. A phenomenological macroscopic model was used to investigate the criteria in a broad-spaced collision-dominated plasma diode. Results were presented that clearly show the effects of volume ionization and/or recombination. Since the electron temperature and the net volume ionization are both treated as independent variables, these results are a parametric family of curves. The envelope of this family of curves is bounded in the $I_s - A_{DE}$ plane. Results were presented in both the $I_s - A_{DE}$ plane and in the $I - A_{DE}$ plane for several cases of interest in thermionic energy conversion. These results are useful in the determination of the emitter sheath polarity from current-voltage characteristics of broad-spaced plasma diodes.

References

1. Talaat, M.E. "The Surface Ionization and Volume Ionization Modes of Operation in the Thermionic Plasma Energy Converter." Advanced Energy Conversion. Vol. 2, (1962), pp. 447-458; Talaat, M.E. "Generalized Theory of the Thermionic Energy Converter," AIEE General Meeting, New York, Jan. 28-Feb. 2, 1962. Paper No. 62-291.
2. Dunlop, J. and Schrenk, G. "Theoretical Model of a Thermionic Converter," Proceedings of the Thermionic Conversion Specialist Conference, Oct. 7-9, 1963, pp. 57-62.

APPENDIX

Consider the derivation of the energy balance equation for the plasma (Equation (6)). The motive diagram under consideration is shown in Figure 1. Choose the potential reference point for both atoms and electrons to be the potential at the emitter surface.

Consider an imaginary surface immediately outside the emitter and look at the energy carried by each species crossing this surface. Thus:

$$\text{Energy carried by electrons emitted} = I_{so}(2V_{TE})$$

$$\text{Energy carried by atoms evaporated from surface} = I_{aE}(2V_{TE})$$

$$\text{Energy carried by ions evaporated from surface} = I_{pE}(2V_{TE} + V_i)$$

$$\text{Energy carried by ions from the plasma} = I_p(2V_G + V_i)$$

$$\text{Energy carried by electrons from the plasma} = I_{ep}(2V_{Te})$$

$$\text{Energy carried by neutral atoms from the plasma} = I_{ap}(2V_G)$$

The net energy crossing this imaginary surface into the plasma is

$$\begin{aligned} & I_{so}(2V_{TE}) + I_{aE}(2V_{TE}) + I_{pE}(2V_{TE} + V_i) - I_p(2V_G + V_i) \\ & - I_{ep}(2V_{Te}) - I_{ap}(2V_G) \end{aligned} \quad (A-1)$$

Consider an imaginary surface immediately outside the collector and look at the energy carried by each species crossing this surface. Thus:

$$\text{Energy carried by neutral atoms from the collector} = I_{ac}(2V_{TC})$$

$$\text{Energy carried by ions from the plasma} = I_p(2V_G + V_i + V_{sc} + V_{ref})$$

$$\text{Energy carried by electrons from the plasma} = I_{ep} \exp(-V_{sc}/V_{Te})(2V_{Te} - V_{ref})$$

$$\text{Energy carried by neutral atoms from the plasma} = I_{ap}(2V_G)$$

where, neglecting plasma resistance, $V_{ref} = (\phi_E - \phi_C) - V = -V_{sc}$.

This arises from the choice of the potential reference point.

The net energy crossing this surface out of the plasma is

$$\begin{aligned} & I_p(2V_G + V_i + V_{sc} + V_{ref}) + I_{ep} \exp(-V_{sc}/V_{Te})(2V_{Te} - V_{ref}) \\ & + I_{ap}(2V_G) - I_{ac}(2V_{TC}) \end{aligned} \quad (A-2)$$

Now, conservation of the number of cesium particles yields

$$\begin{aligned} I_{aE} + I_{pE} &= I_p + I_{ap} = I_a \\ I_{aC} &= I_p + I_{ap} = I_a \end{aligned} \quad (A-3)$$

Neglecting extraneous losses, the net energy entering the plasma at the emitter surface must equal the net energy leaving the plasma at the collector surface. Thus, equating (A-1) and (A-2) and using Equations (A-3), it follows that

$$\begin{aligned} I_{so}(2V_{TE}) + I_a(2V_{TE} + 2V_{TC} - 4V_G) + V_i(I_{pE} - 2I_p) \\ - I_{ep}(2V_{Te}) - I_{ep} \exp(-V_{sc}/V_{Te})(2V_{Te} + V_{sc}) = 0 \end{aligned} \quad (A-4)$$

Substituting Equations (1), (2), and (3), and rearranging terms, Equation (A-4) reduces to

$$\begin{aligned} 2I_{so}(V_{TE} - V_{Te}) + 2I_a(V_{TE} + V_{TC} - 2V_G) \\ - A_{DE}(V_i + 2V_{Te}) - (I + I_p)V_{sc} = 0 \end{aligned} \quad (A-5)$$

This is the energy balance equation for the plasma (Equation (6)). Through proper choice of the potential reference point and through the use of the equality of the energy fluxes crossing the imaginary surface at the emitter and the collector, all interactions that take place in the interelectrode space have been taken into account. There is no need to introduce detailed interaction mechanisms to evaluate any of the terms occurring in this energy balance equation.

MOTIVE DIAGRAM

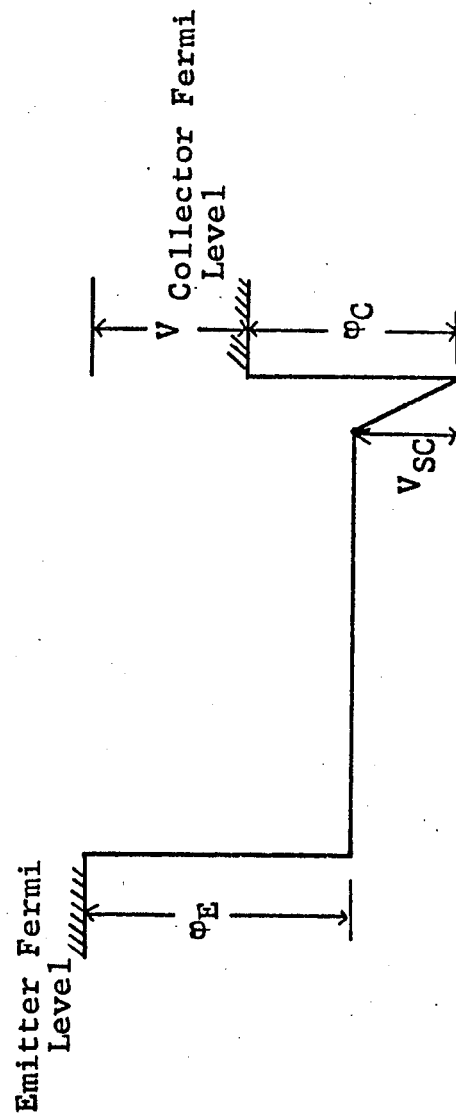


Figure 1. Motive diagram for a zero emitter sheath.

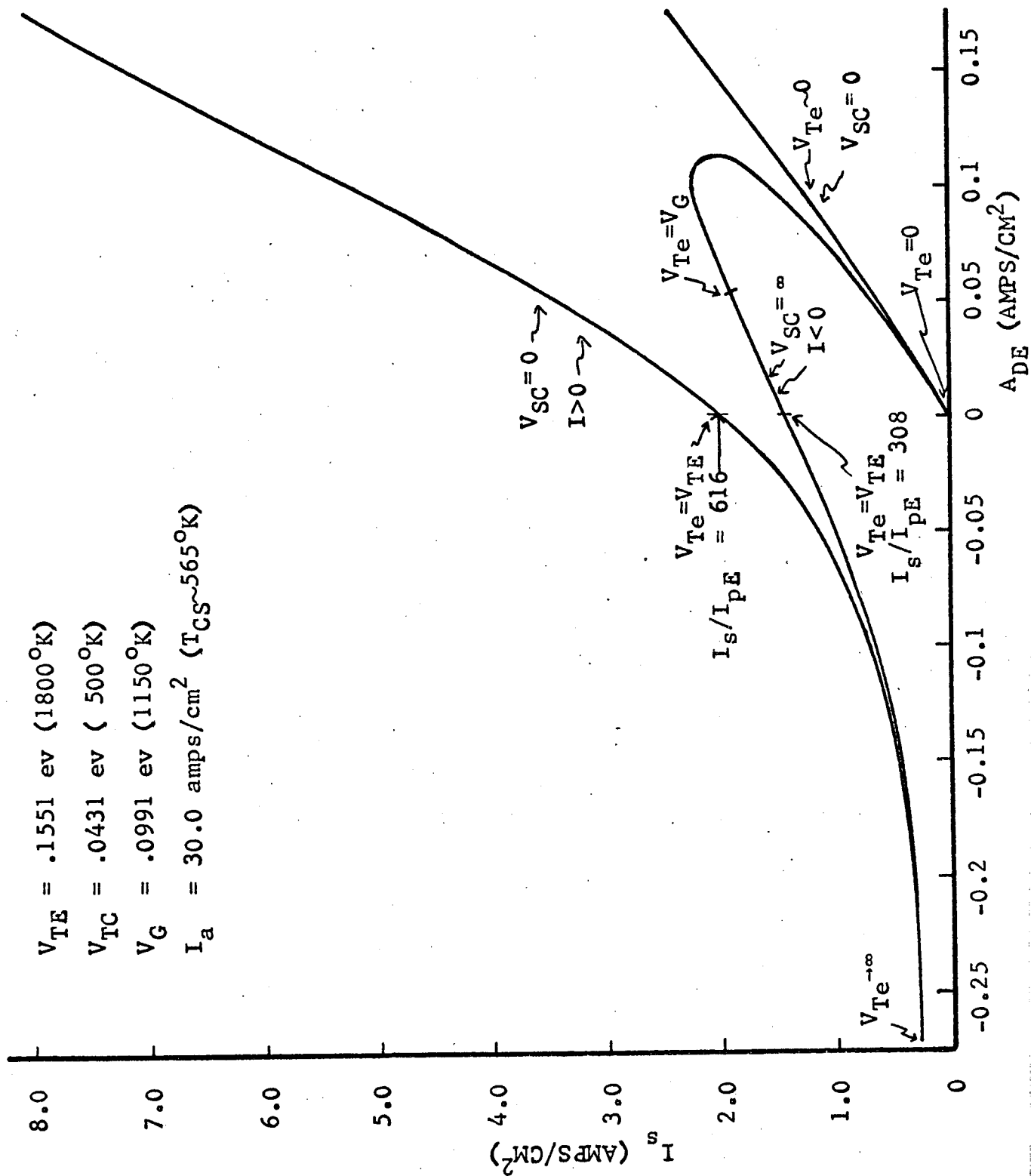


Figure 2. Envelope of zero emitter sheath solutions for $0 \leq V_{Te} \leq \infty$.

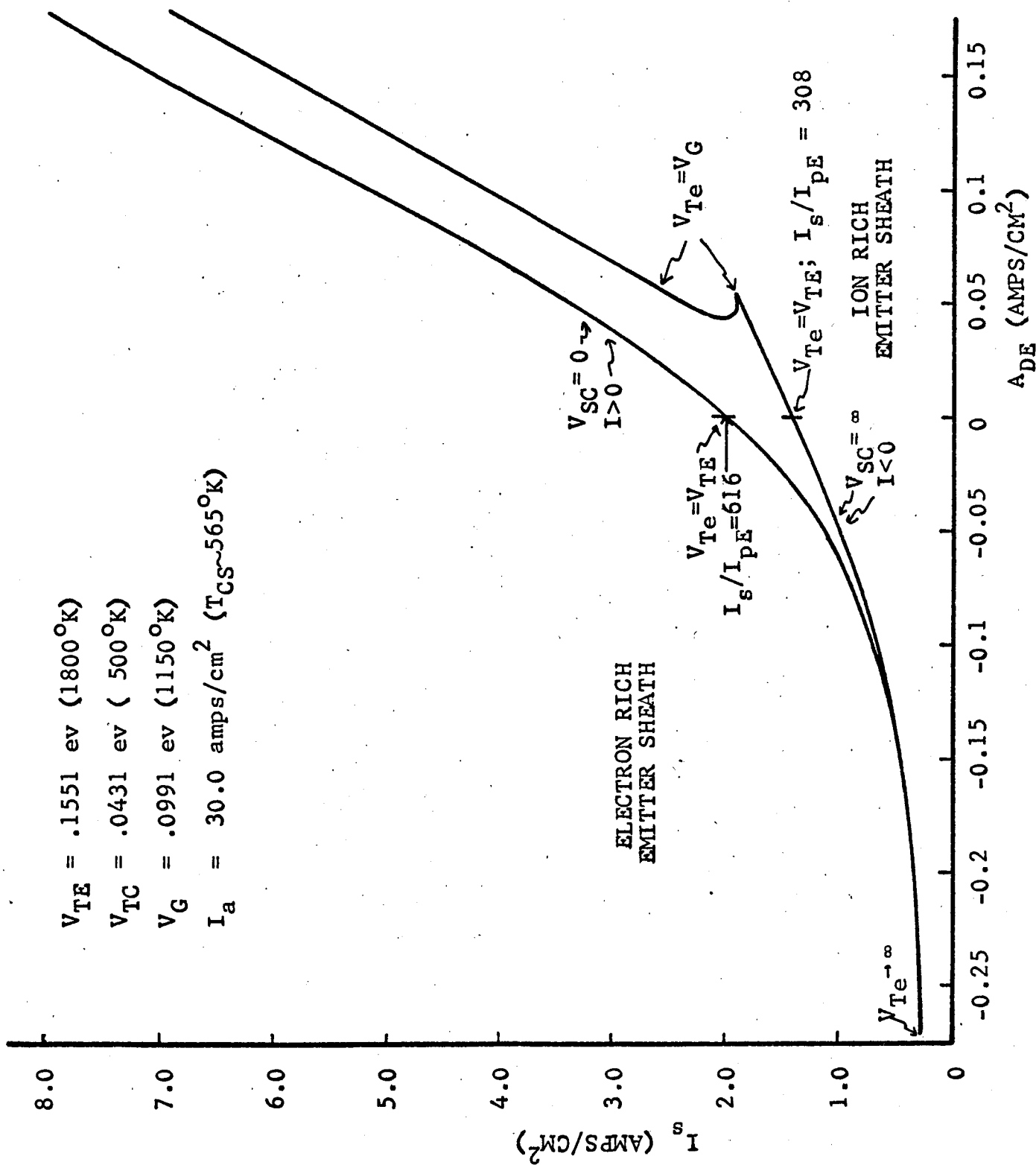


Figure 3. Envelope of zero emitter sheath solutions for $V_G \leq V_{Te} \leq \infty$.

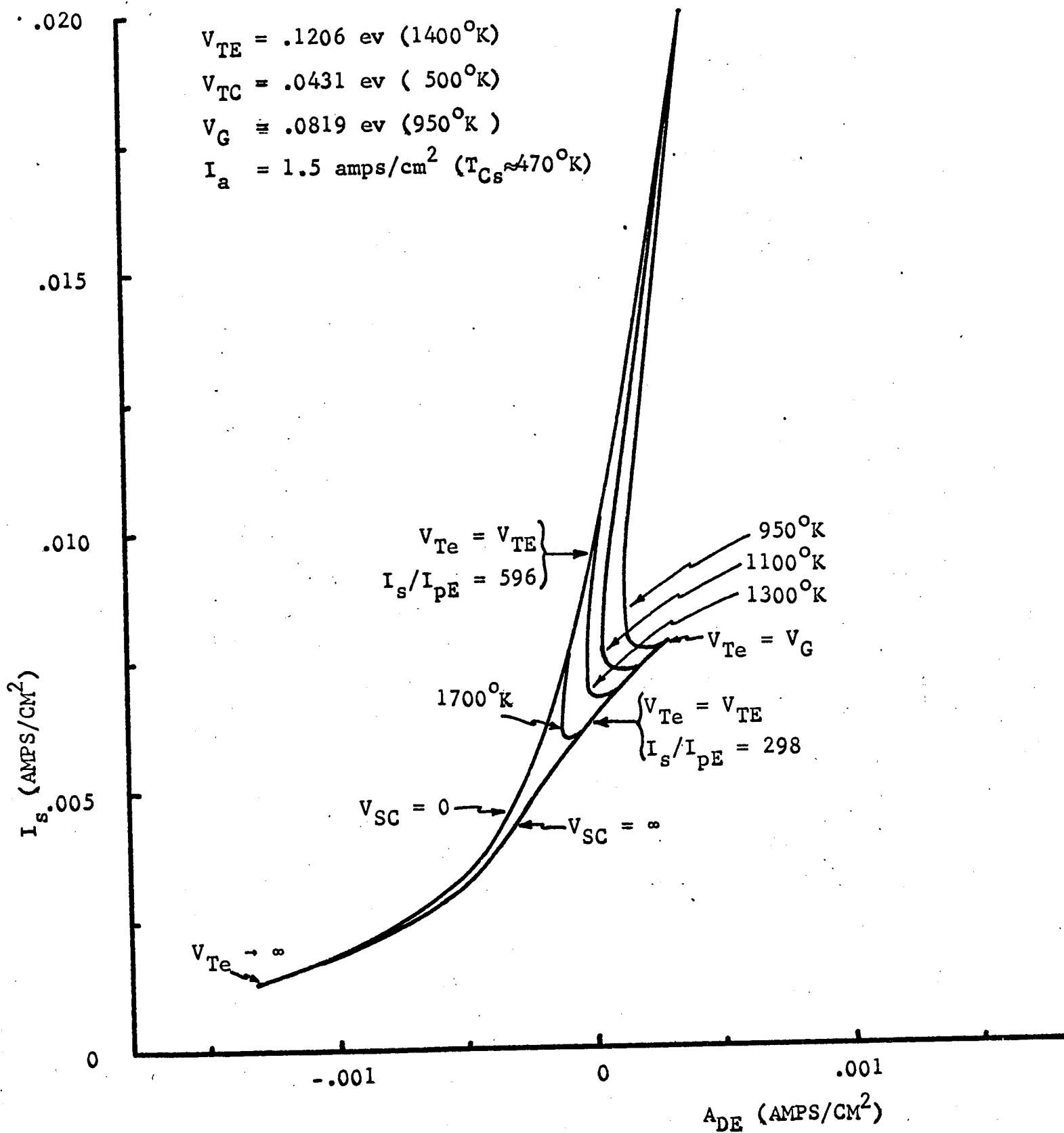


Figure 4.

$V_{TE} = .1249 \text{ ev (1450}^\circ\text{K)}$
 $V_{TC} = .0431 \text{ ev (500}^\circ\text{K)}$
 $V_G = .0840 \text{ ev (975}^\circ\text{K)}$
 $I_a = 1.5 \text{ amps/cm}^2 \text{ (} T_{CS} \approx 470^\circ\text{K)}$

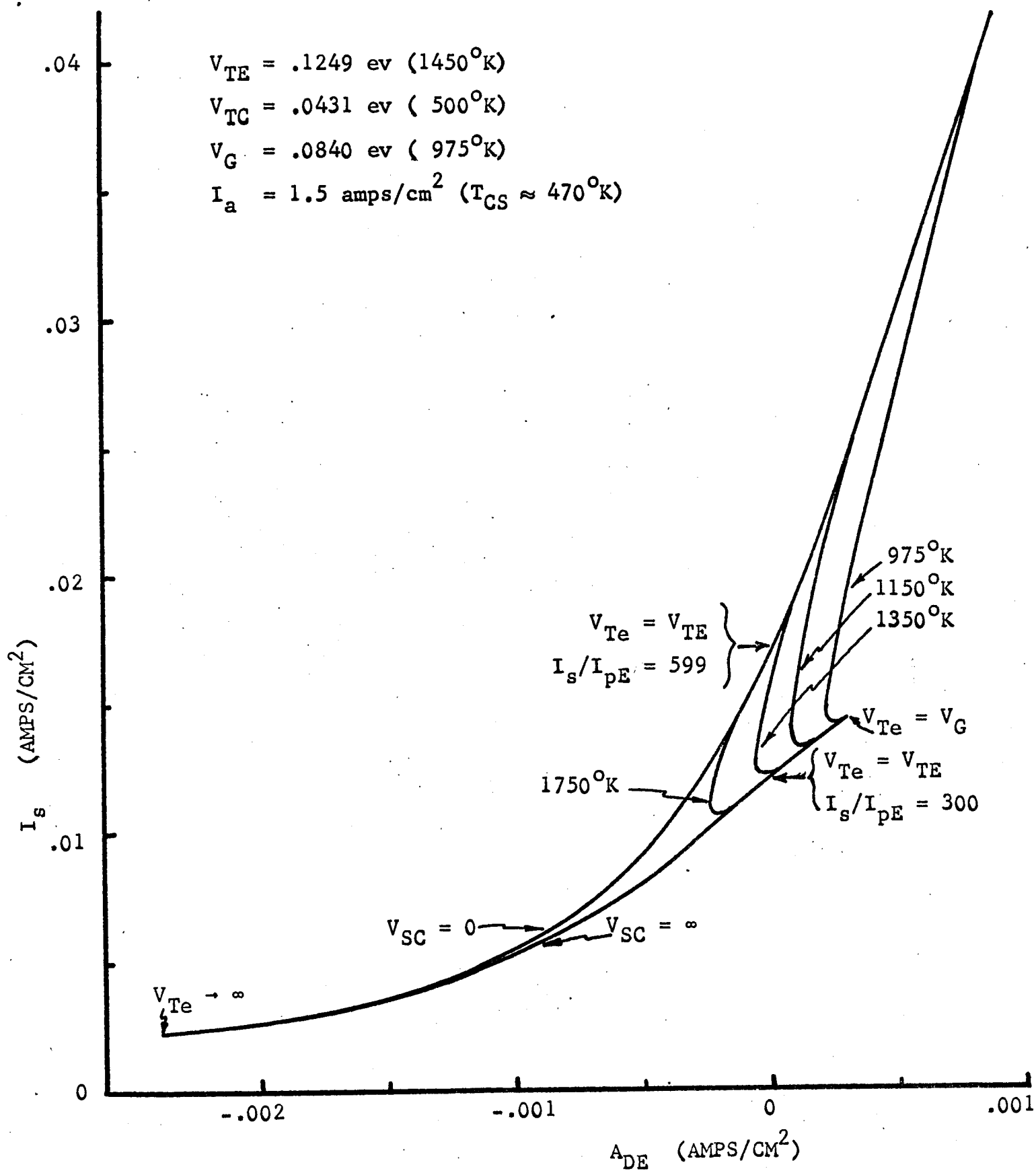


Figure 5.

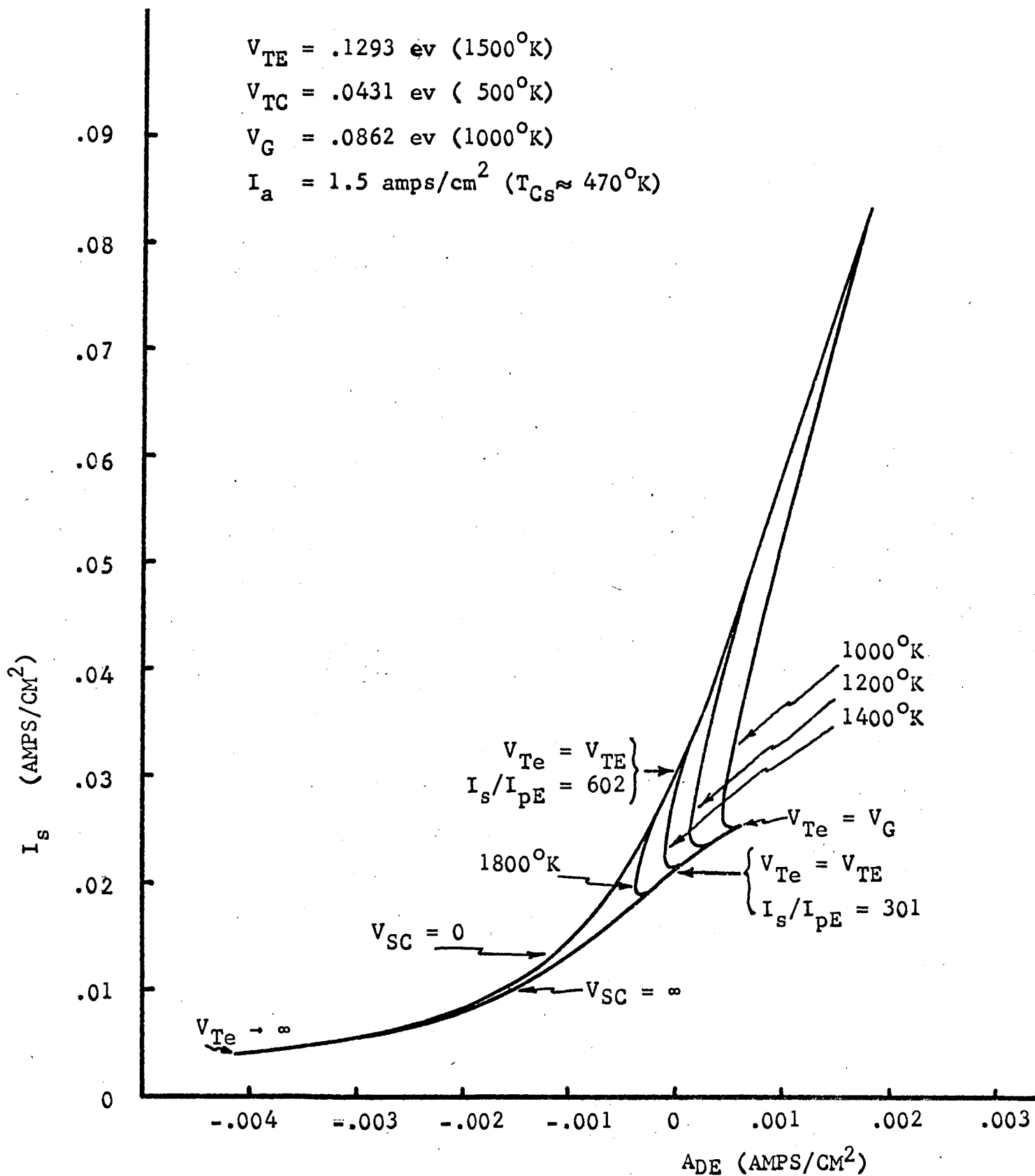


Figure 6.

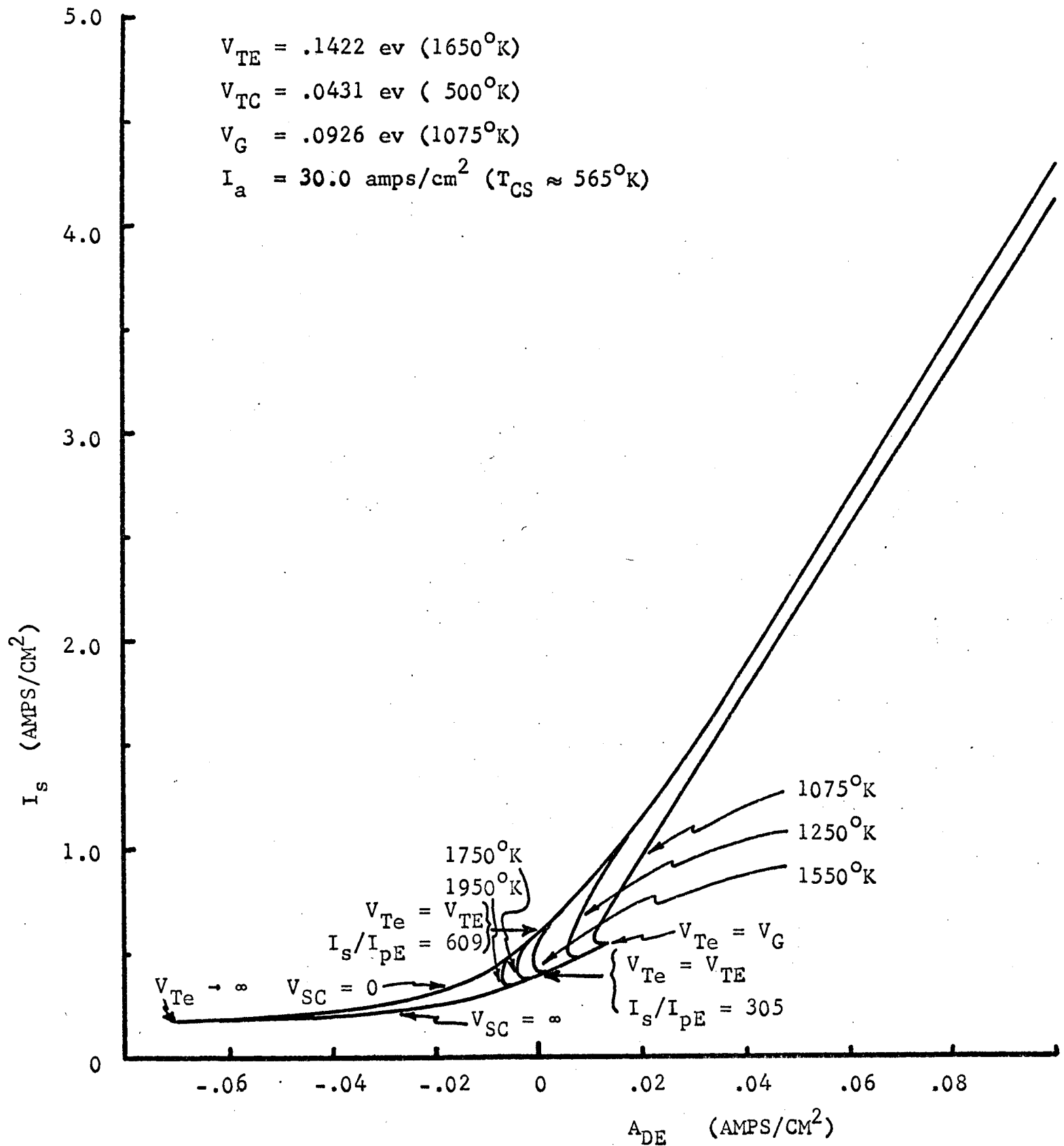


Figure 7.

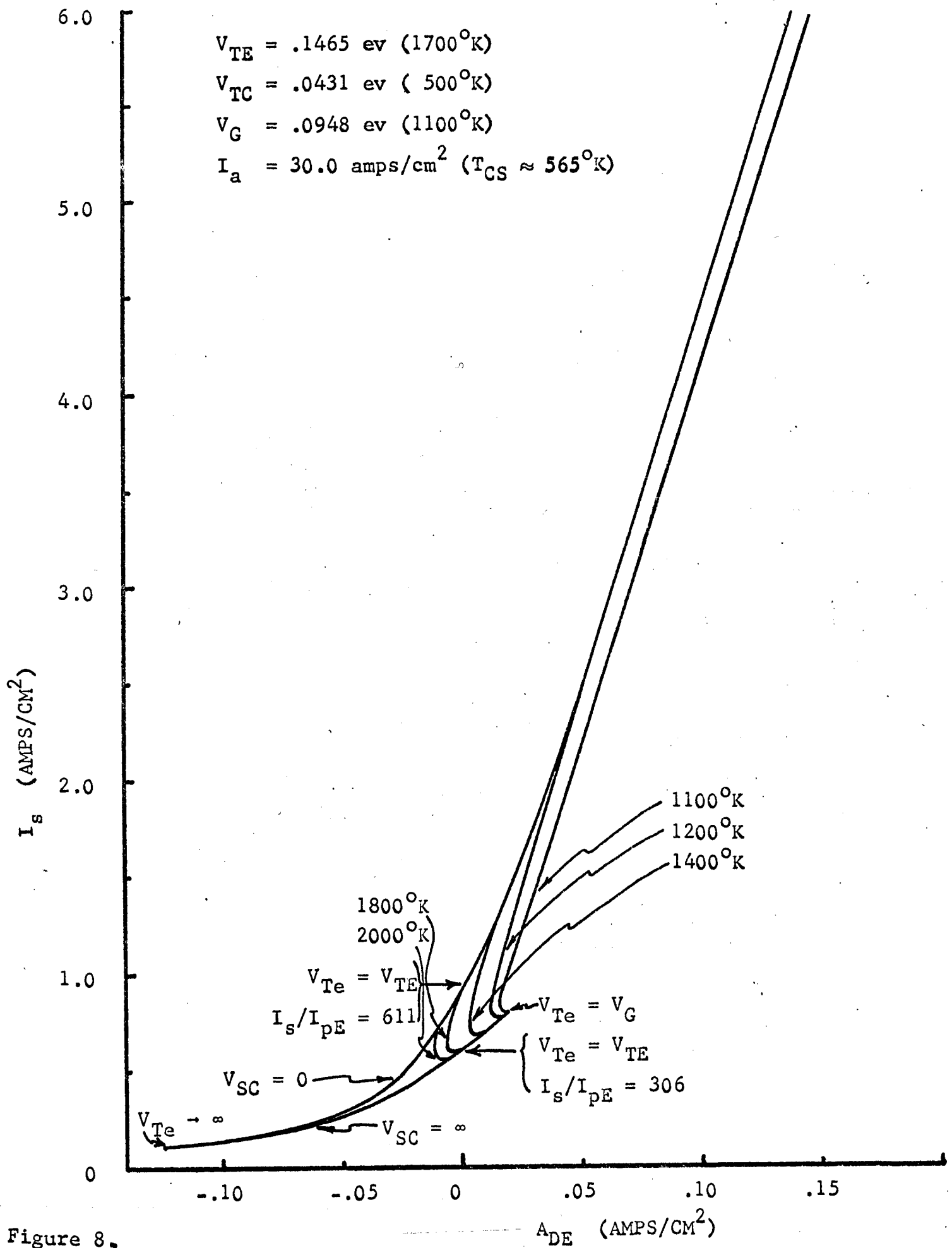


Figure 8.

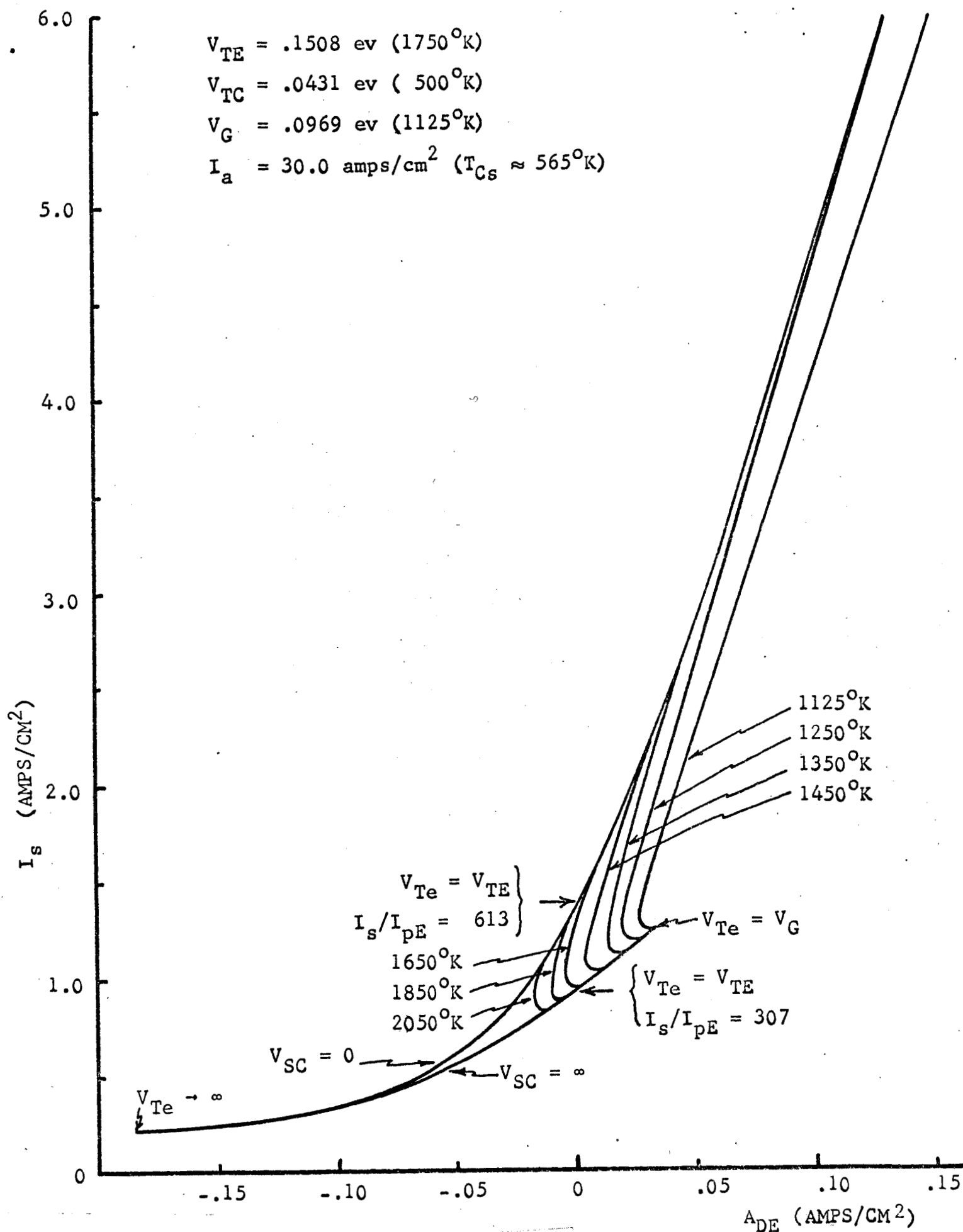


Figure 9.

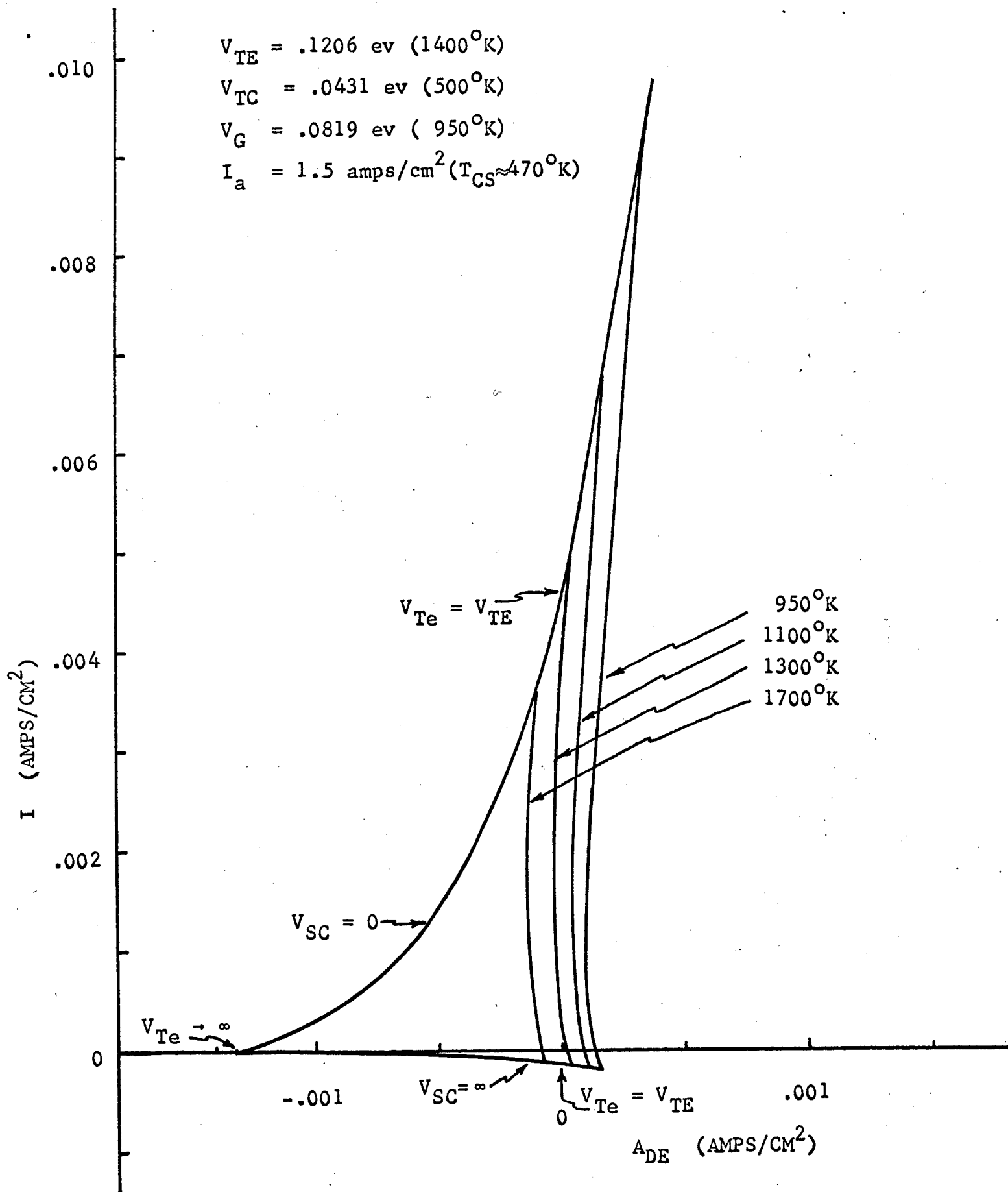


Figure 10.

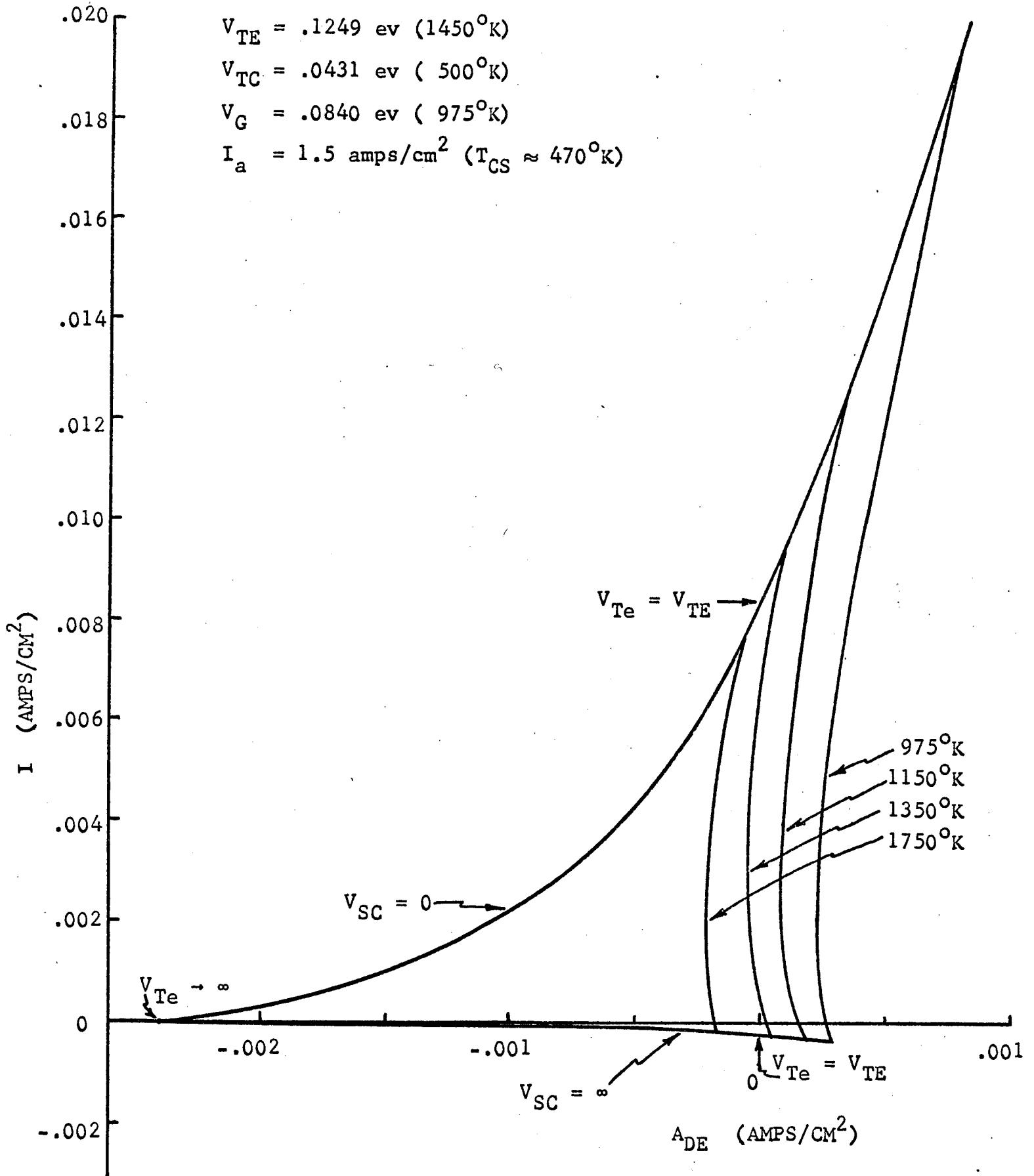


Figure 11.

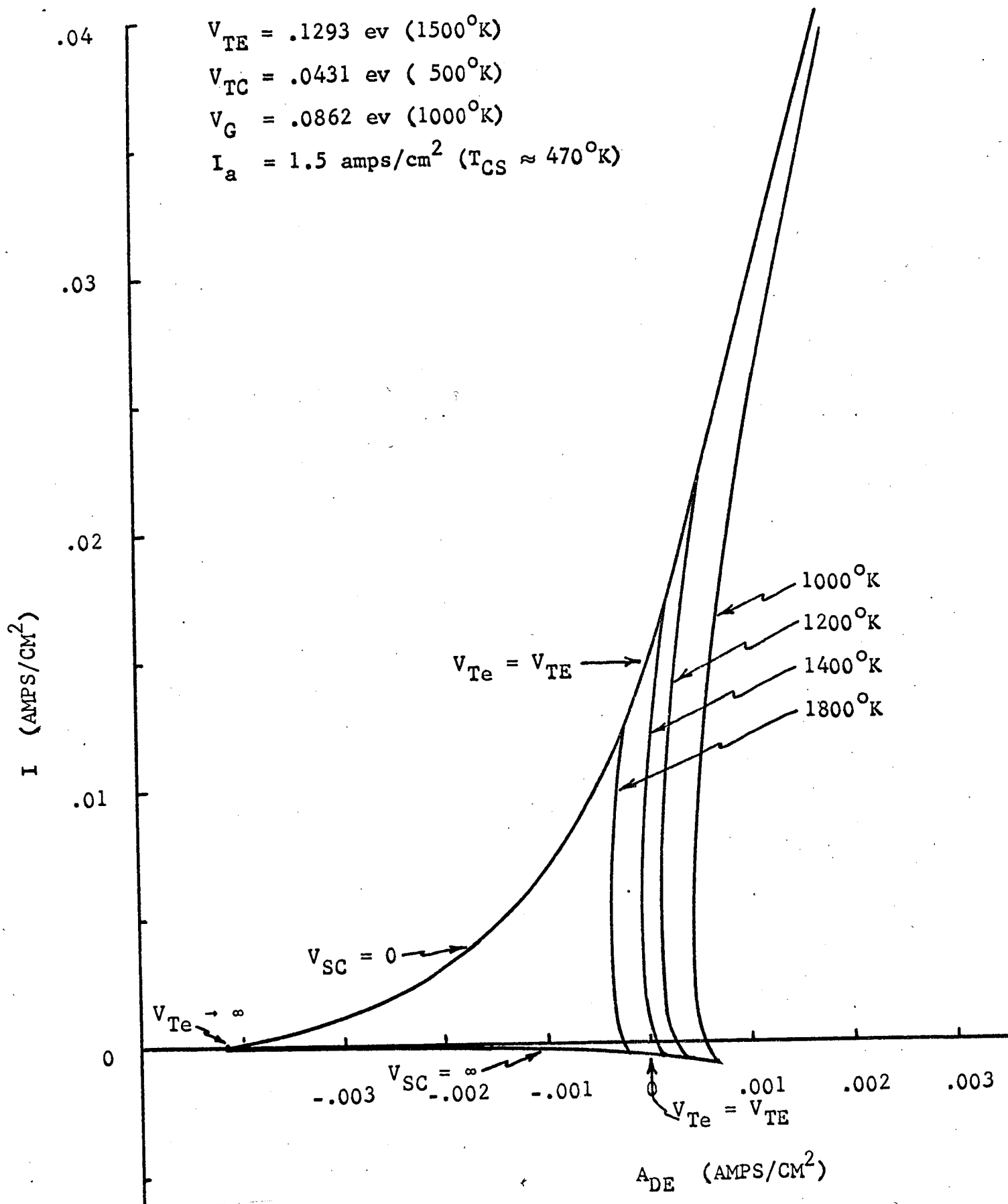


Figure 12.

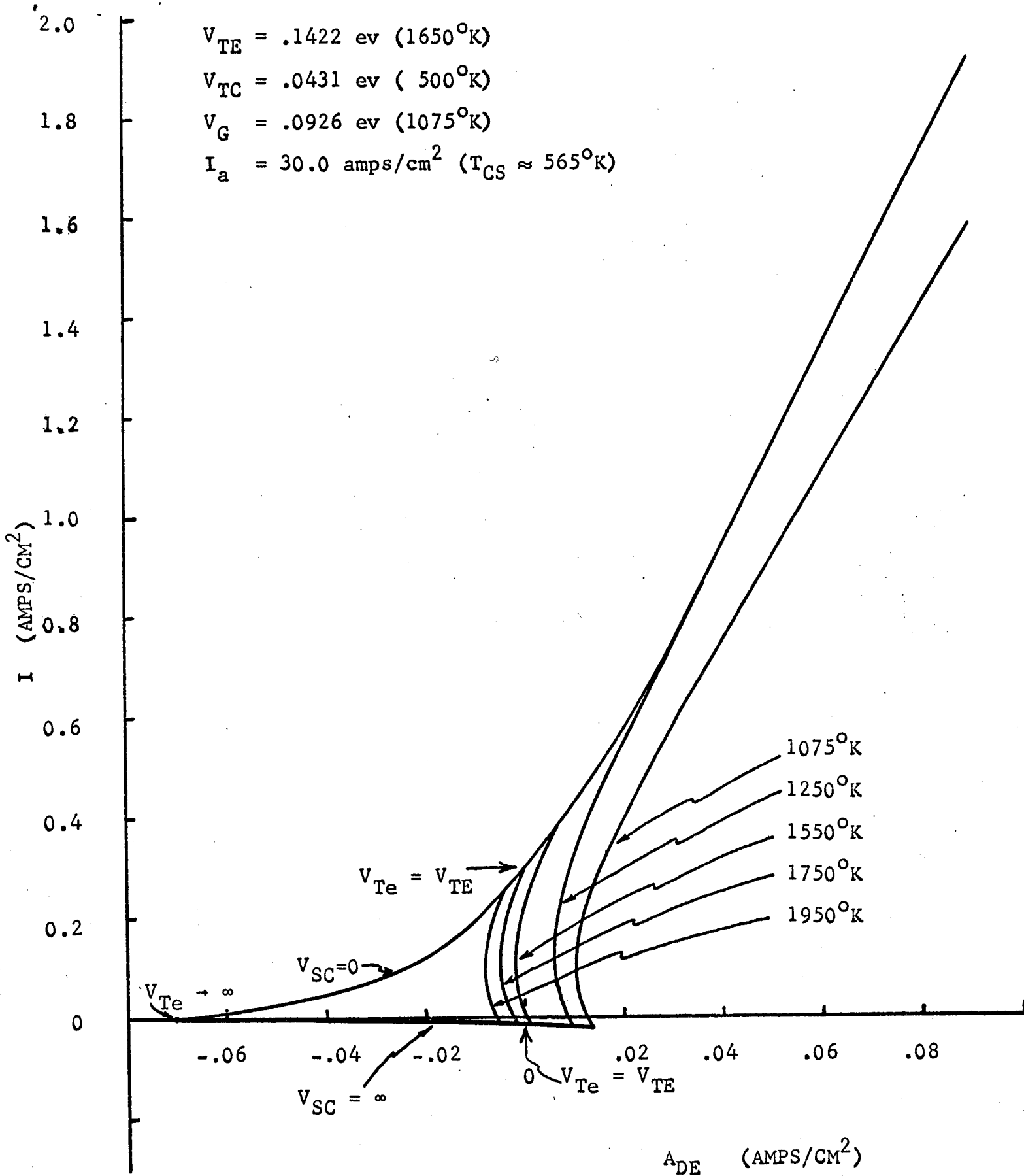


Figure 13.

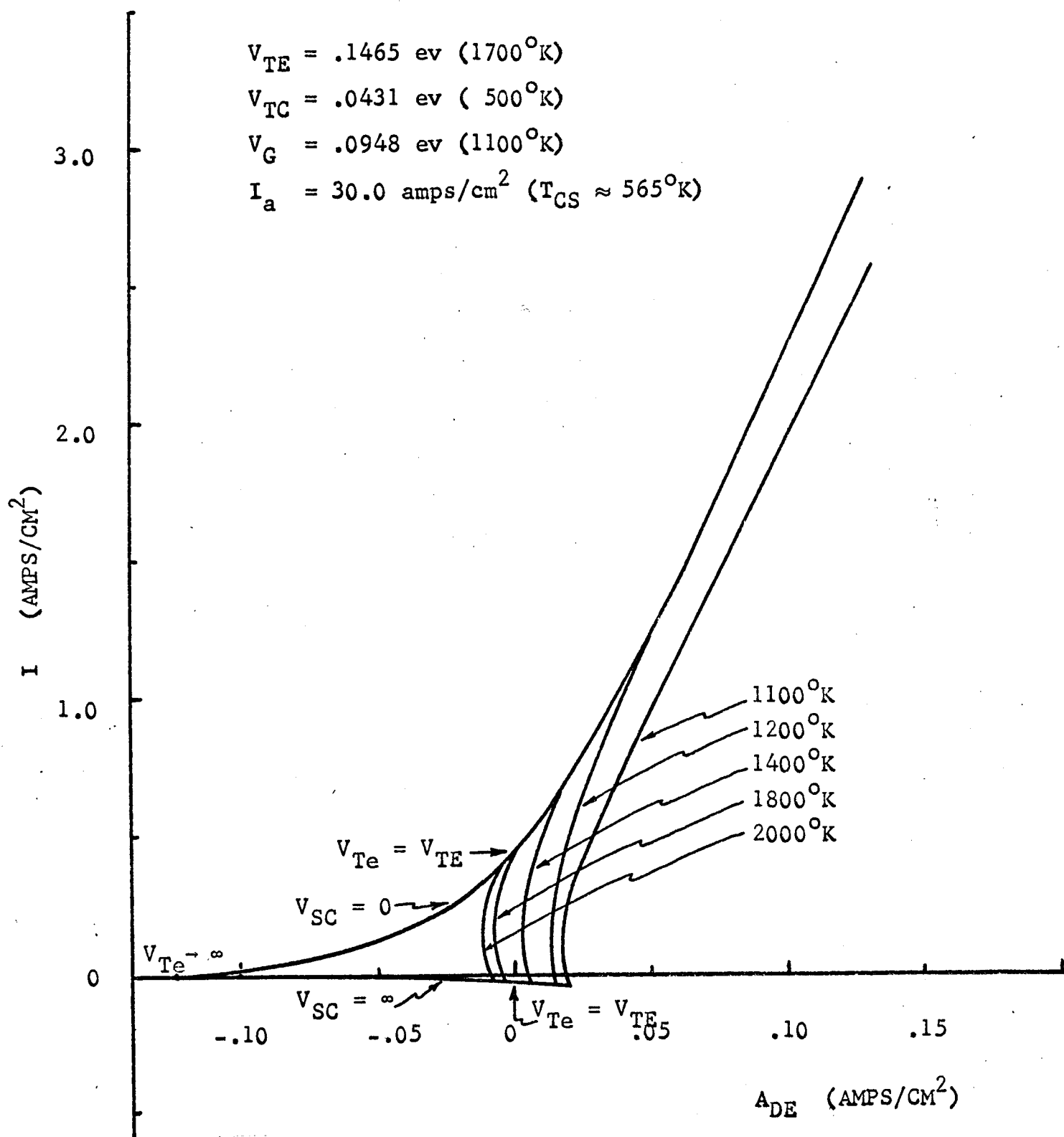


Figure 14.

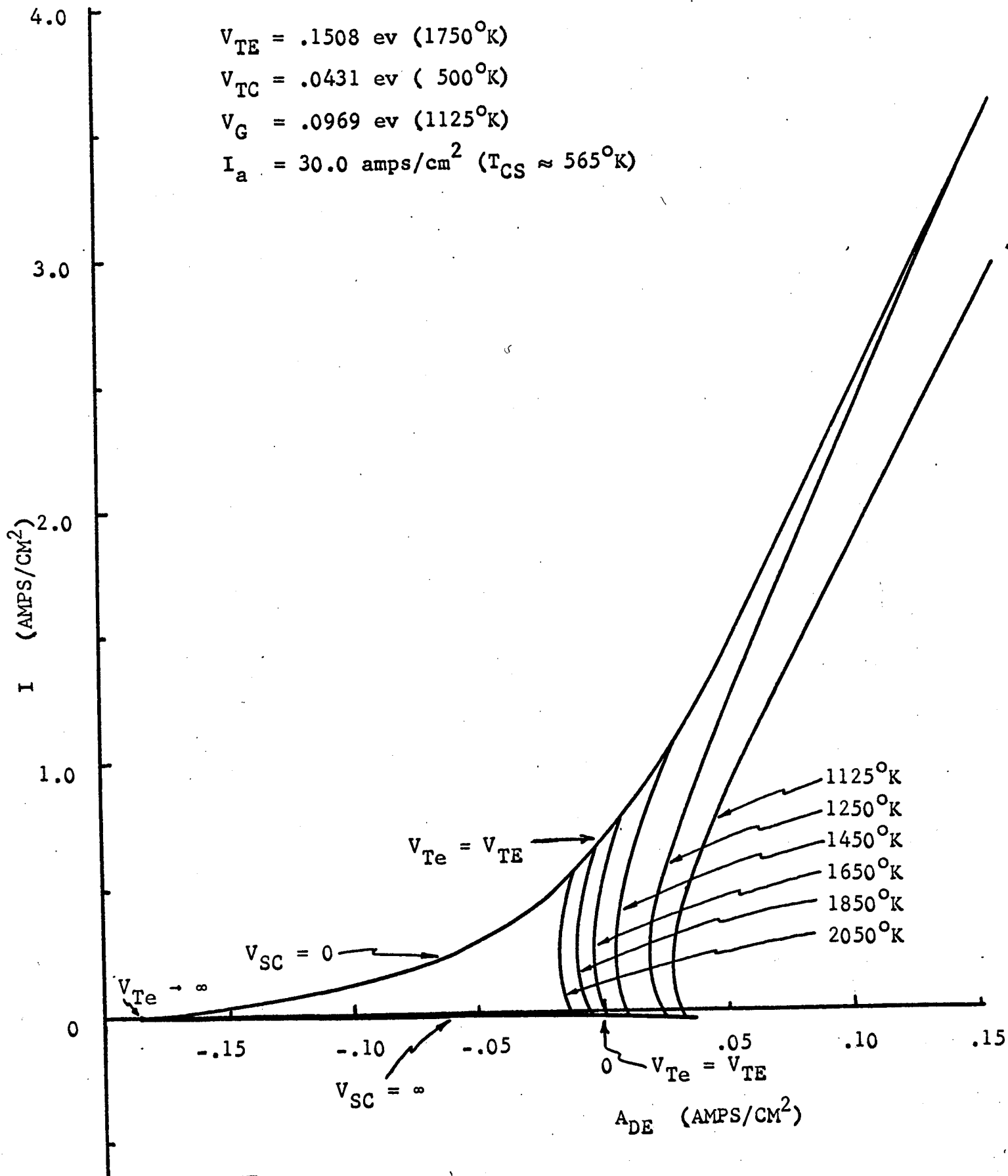


Figure 15.